PCCP

The Properties of Irn(n=2-10) Clusters and its Nucleation on γ-Al2O3 and MgO Surface: From ab initio studies

Journal:	*Physical Chemistry Chemical Physics*
Manuscript ID:	CP-ART-10-2014-004881.R1
Article Type:	Paper
Date Submitted by the Author:	17-Nov-2014
Complete List of Authors:	chen, yongchang; Nanchang Hangkong University, huo, miao; Nanchang Hangkong University, chen, tong; Nanchang Hangkong University, li, qiang; Liaoning shihua University, sun, zhaolin; Liaoning shihua University, song, lijuan; Liaoning shihua University,

SCHOLARONE™
Manuscripts

The Properties of Ir$_n$(*n*=2-10) Clusters and its Nucleation on

γ-Al$_2$O$_3$ and MgO Surface: From *ab initio* studies

Yongchang Chen[1]   Miao Huo[1]   Tong Chen[1]   Qiang Li[2]   Zhaolin Sun[2]   Lijuan

Song[2*]

[1.] Nanchang Hangkong University, Nanchang 330063, China

[2.] Liaoning Key Laboratory of Petrochemical Catalytic Science and Technology, Liaoning Shihua University, Fushun 113001, China

* E-mail address: chenyc828@foxmail.com；lsong56@foxmail.com

Tel: 0086-791-83863131; Fax: 0086-791-83863145

ABSTRACT

The structural, stability, and magnetic properties of iridium clusters Ir$_n$ (*n*=2−10) and its interaction on γ-Al$_2$O$_3$ (001) and MgO(100) Surface have been investigated from first principles calculations. It is found that the adsorption energy of Ir$_n$(*n*=2-10)/γ -Al$_2$O$_3$(001) is lower than that of Ir$_n$/MgO(100), meanwhile, the strongest adsorption energy cluster for γ-Al$_2$O$_3$(001) is the tetrahedral Ir$_4$ cluster, while MgO(100) is a cubic structure Ir$_8$ cluster. On the other hand, the nucleation of Ir$_n$(*n*=2-10) cluster on both surface are thermodynamically favorable and exothermic. Moreover, the nucleation energy of Ir$_n$(*n*=2-10) cluster on the γ-Al$_2$O$_3$(001) surface is close to the corresponding energy on the MgO(100) surface, except for Ir$_3$, Ir$_4$ and Ir$_6$ cluster. Interestingly, the nucleation of Ir$_3$ and Ir$_6$ cluster on MgO(100) surface are more favorable than that on the γ-Al$_2$O$_3$(001) surface, while the nucleation of Ir$_4$ cluster is

reverse and very close to the gas phase Ir_4 cluster. More importantly, deformation energy and charge density analysis show that the adsorbed Ir_4 cluster on the γ-Al_2O_3(001) surface has obviously charge transfer between Ir atoms and surface Al, O atoms with negligible deformation. However, for the MgO(100) surface, the Ir_4 cluster connect directly to three surface O atoms with severe distortion, which inhibit the activity of the tetrahedral Ir_4 cluster as a catalyst.

Keywords: Ir_n (n=2-10) cluster; Oxide surface; Adsorption; Nucleation; Charge density; *ab initio*

1. INTRODUCTION

Oxide-supported metal Catalysts are one of the most important factors that have largely speed up the developments in petroleum and chemical industries.[1] For heterogeneous catalysis, supported metal atoms or clusters play a pivotal role in industrial catalytic processes.[2-3] The active species of dispersed metal catalysts are often small clusters, and their catalytic activities are differ from bulk metal or low index metal surfaces.[4] Many supports have been used to disperse iridium particles in surface science studies, such as MgO,[5-6] γ-Al_2O_3[7-8] and TiO_2.[9]

In this paper, we focus on the structure of small Ir clusters on γ-Al_2O_3 surfaces and MgO surfaces. Heterogeneous catalysts containing iridium clusters on different supports have been examined in a number of previous experimental and theoretical studies.[5-11] Argo et al. investigated

the hydrogenation reactions of ethene, propene, and toluene on small clusters of iridium (Ir_4 and Ir_6) on oxide supports (γ-Al_2O_3 and MgO). By using extended X-ray absorption fine structure (EXAFS) spectroscopy, their providing evidence of the cluster structures and cluster-support interactions in the working state. Moreover, the experimental date indicated that the catalytic activity of the iridium clusters for alkene hydrogenation reactions is tenfold boosted when γ -Al_2O_3 is used, instead of MgO, as the support.[12] It has been generally accepted that the catalytic activity of catalysts is very sensitive to both of the metal cluster size and the support material. [10-15]

Under laboratory conditions, little information is available in the literature concerning the complete structural and electronic information for metal clusters on metal oxide supports because of the structural complexity of metal clusters. First principles calculations have demonstrated their powerful capability not only of illustrating the structure but also of predicting the catalytic activity of material for heterogeneous catalyst.[16-19] Theoretical approaches based on first-principles calculations are useful to complement experimental results. Many studies have investigated the nucleation and growth of transition metals on Oxide supports, including Pd on γ -Al_2O_3,[20] Rh on γ -Al_2O_3[21] and Cu on γ -Al_2O_3.[22] To our knowledge, little attention has been paid to nucleation and growth of Ir on γ-Al_2O_3 surfaces or MgO surfaces.

Moreover, motivated by the different catalytic activity between the support γ-Al$_2$O$_3$ and MgO which observed by Argo et al.[12] We present a systematic theoretical investigation about the stability and nucleation of small Ir$_n$(n=1–10) clusters on the support γ-Al$_2$O$_3$ and MgO surfaces by using density functional theory method.

The aim of this study have the following three points: 1) to determine the structures and properties of Ir$_n$ clusters (n=2-10); 2) to identify the preferred adsorption site and the properties of isolated Ir$_n$ clusters after the adsorption on the different surfaces; 3) to compare the stability and nucleation of Ir$_n$ clusters for the γ-Al$_2$O$_3$ and MgO support.
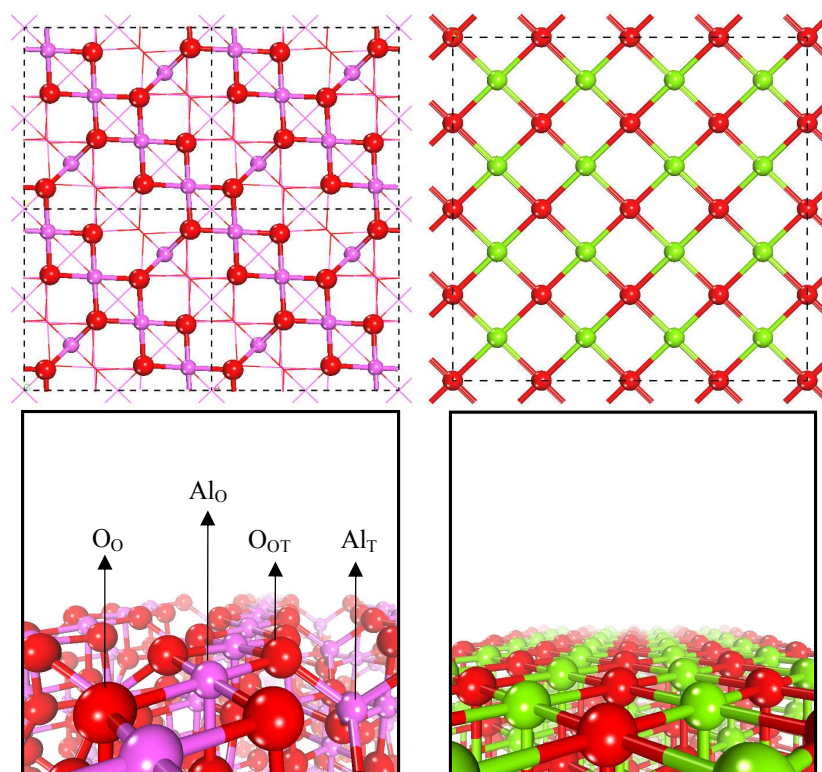
Figure 1. Top and side view of the γ-Al$_2$O$_3$(001) surface (left) and MgO(100) surface (right), pink, red and green sphere stand for Al, O and Mg atoms, respectively.

2. COMPUTATIONAL   DETAILS

All calculations reported herein were performed with plane-wave density functional theory(DFT) using the VASP (Vienna ab initio simulation package) code.[23-24] The projector augmented wave (PAW) method with PW-91 exchange-correlation functional was used to model the core electrons. Ir $5d^8$ and $6s^1$, O $2s^2$ and $2p^4$, Al $3s^2$ and $3p^1$, Mg $3s^2$ electrons are treated as valence electrons, while all the other electrons are treated as core electrons.[25] A cutoff of 380 eV was employed for the plane-wave expansion of the wave function, and spin polarization was used for all calculation.

As shown in Fig.1, the γ -Al$_2$O$_3$(001) structural models based on defective spinel model are constructed according to our previous work.[26] The slab is consisted of 48 O atoms, 32 Al atoms and 2 octahedral site vacancies lies in the middle of the slab, including eleven layers. In order to ignore the electrostatic interactions between the two surfaces in the slab, the vacuum layer should be thick enough, and the slab separated in z direction was defined as 12 Å. On the other hand, for the MgO(100) structural models, to avoid lateral interactions between the periodic Ir clusters, a slab containing 4 ×4 unit cells in the plane of the surface, including five layers was adopted, and the spacing between the adjacent slabs (along z-direction) was also set at 12 Å. The supercell for γ-Al$_2$O$_3$(001) and MgO(100) surfaces contained 80 and 180 atoms,

respectively. The convergence of the total energy with respect to the k-points sampling were carefully examined and finally 3×3×1 (for γ -Al$_2$O$_3$(001)) and 2×2×1 (for MgO(100)) Monkhorst-Pack scheme k-point meshes are used for the k-points sampling in the Brillouin zone.[27] For relaxation of Ir cluster adsorbed on the surface, all atoms were fully relaxed until the final forces on all the relaxed atoms were smaller than 0.05 eV/Å.

In this paper, we reported the most stable adsorption configurations of Ir$_n$(n=1-10) cluster adsorption on support surface. The adsorption energy of Ir cluster was defined by the following Equation:

$$E_{ads} = E(Ir_n) + E(slab) - E(Ir_n/slab) \qquad (1)$$

Where E(Ir$_n$), E(slab), and E(Ir$_n$/slab) are the total energies of the isolated Ir$_n$ cluster, the bare slab(γ -Al$_2$O$_3$(001) or MgO(100), and the slab with Ir$_n$ cluster. The E_{ads} can be divided into two components to investigate the chemisorption process. The deformation energy for Ir$_n$ cluster was calculated by using:

$$E_{def(Irn)} = E(Ir_n') - E(Ir_n) \qquad (2)$$

where E(Ir$_n'$) is the total energy of adsorbed Ir$_n$ cluster in the gas phase. Similarly, the surface deformation energy was calculated as following:

$$E_{def(surface)} = E(slab') - E(slab) \qquad (3)$$

where E(slab$'$) is the total energy of the deformed slab after adsorbed Ir$_n$ cluster. Moreover, we also calculated the cluster support interaction

energy by using

$$E_{int} = E(Ir_n') + E(slab') - E(Ir_n/slab) \tag{4}$$

where E_{int} uses energies for the separated clusters and substrate in the geometry associated with the fully relaxed adsorbed cluster. Therefore, the adsorption energy can be conclude as following equation:

$$E_{ads} = E_{int} - E_{def(Irn)} - E_{def(surface)} \tag{5}$$

Obviously, the adsorption energy is a trade-off between deformation energy and cluster support interaction energy. To obtained the stability of Ir_n cluster, the average binding energy of isolated $Ir_n(n=1-10)$ cluster in the gas phase was calculated by following equation:

$$E_{b(Irn)} = [n \times E(Ir) - E(Ir_n)]/n \tag{6}$$

Similarly, the binding energy of $Ir_n(n=1-10)$ cluster adsorbed on surface was depicted as following equation:

$$E_{b(Irn/slab)} = [E(Ir_n/slab) - n \times E(Ir) - E(slab)]/n \tag{7}$$

where $E_{b(Irn/slab)}$ represent the stability of $Ir_n(n=1-10)$ cluster adsorbed on surface.

3. RESULTS AND DISCUSSION

3.1 Structures of $Ir_n(n=2-10)$ Cluster in the Gas Phase
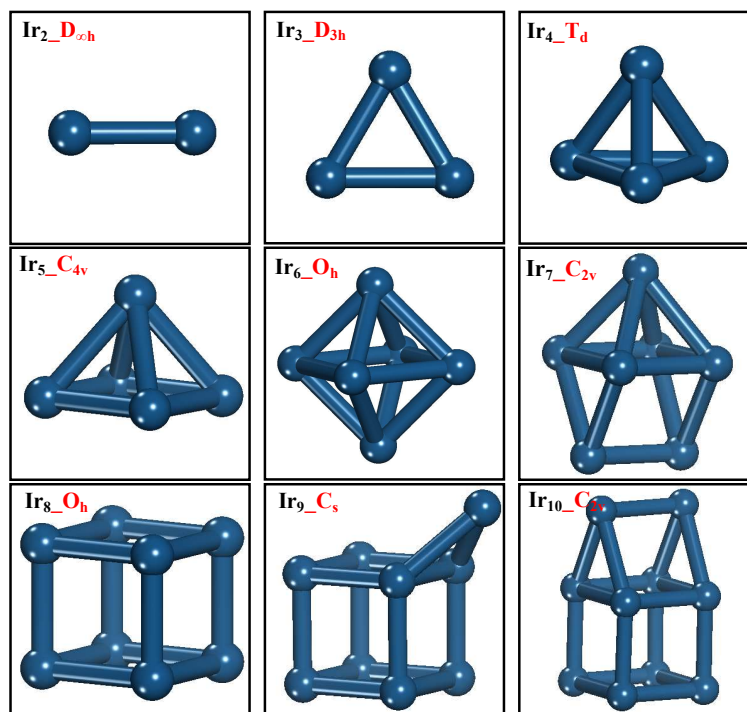
Figure 2. The optimized low energy geometry for adsorption with number labels of Ir_{2-10} clusters.

To understand the stability and growth behavior of $Ir_n (n=1-10)$ on surface, different isomers of small Iridium clusters in the gas phase have been investigated. According to the energy from low to high, the energetically preferred geometries were obtained. The molecular properties of these geometries, coordination numbers (CN), atomic magnetic moments (M/atom), binding energy per atom (E_b/atom) and average bond lengths (R_{ave}), are calculated in Table 1. For the sake of simplicity, we only present the isomers with low energy for discussion. The low energy geometries with number labels for $n=2-10$ are listed in Fig.2, which are also used for further adsorption.

Table 1. Geometry, Coordination Numbers (CN), Magnetic Moment (Mag), Binding Energy(E_b/atom) and Average Bond Lengths (R_{ave}) of low energy Gas Phase Ir$_n$ ($n = 2-10$) Clusters

n	geometry	CN	Mag(μ_b)	E_b/atom(eV)	R_{ave}(Å)
2	$D_{\infty h}$	1	4	2.613	2.211
3	$D_{\infty h}$	1.33	1	3.271	2.183
	D_{3h}	2	3	3.190	2.368
4	D_{4h}	2	4	3.853	2.310
	T_d	3	0	3.537	2.462
5	C_{4v}	3.2	5	4.080	2.467
6	D_{3h}	3	6	4.449	2.422
	O_h	4	12	4.332	2.538
7	C_{2v}	3.7	11	4.560	2.506
8	O_h	3	0	5.001	2.371
9	C_s	3.1	3	4.998	2.393
10	C_{2v}	3.4	2	5.146	2.422

The total binding energy of Ir$_2$ dimer in the present work is 5.226 eV, which is in accord with values of 5.06 eV obtained by Pawluk et al.[28] at the PW91 level with the VASP program. Jules et al.[29] obtained the bond length of Ir$_2$ dimer was 2.23 Å by fit of force constants with dissociation energies, which agrees well with our calculated 2.211 Å.

For Ir$_3$ cluster, the ground state of Ir$_3$ is a linear (D$_{\infty h}$) configuration. The lowest energy bent Ir$_3$ structure is a D$_{3h}$ equilateral triangle, which is similar with the Fe$_3$ and Ni$_3$ trimers.[30] The energy for D$_{3h}$ structure is predicted to be 0.243 eV higher than the linear structure.

The lowest energy structure of Ir$_4$ is predicted to be a planar square molecule (in D$_{4h}$) with atomic magnetic moment of 4μ_b. The lowest tetrahedral singlet structure is calculated to be 1.261eV higher than the square planar structure in D$_{4h}$ symmetry. Generally, the cluster Ir$_4$ which

acts as catalyst may still favor T_d configuration with spin singlet. For hydrocarbon hydrogenations, the cluster Ir_4 with T_d point group on solid support Al_2O_3 which possesses catalytic activity was observed.[31] For Ir_5 cluster, the most stable configuration is a square pyramid. The average Ir–Ir bond length and magnetic moment are 2.467Å and $5\mu_b$, respectively. These data are in good agreement with theory results at the BPW91 level with the $Dmol^3$ package by Du et al.[32]

The lowest-energy geometry of Ir_6 cluster favors a triangular prism with D_{3h} point group. The average Ir–Ir bond length and total magnetic moment are 2.422Å and $6.0\mu_b$, respectively. The O_h octahedron structure of Ir_6 is predicted to be 0.704 eV higher than triangular prism. Experimentally, the octahedron Ir_6 that commonly exists in Ir_6 complexes, for the cluster $Ir_6(CO)_{15}^{2-}$ involving in hydrocarbon hydrogenation, the experimental (EXAFS) value shown that the cluster Ir_6 with O_h symmetry on MgO support.[33]

The most stable configuration of Ir_7 is a side-face-capped triangular prism (C_{2v}) structure with coordination numbers of 3.7 and average Ir–Ir bond length of 2.506Å, which are in agreement with the previous results by Dixon et al.[34]

A perfect nonmagnetic cubic structure (O_h) was found to be the most stable structure for Ir_8 cluster. The optimized average bond length(2.371 Å) in present work have a good agreement with previous calculated

values by Zhang et al.[35] The binding energy is as large as 5.001 eV, even bigger than that of Ir_9 cluster(4.998eV), suggesting the outstanding stability of cubic structure of Ir_8 cluster.

For Ir_9 cluster, a C_s point group with Coordination Numbers of 3.1. The average Ir-Ir bond length and average atomic moment are 2.393 Å and $0.33\mu_b$/atom, respectively. The Ir_{10} cluster with Ir_2 dimer capped on the face of cube was found to be the lowest-energy structure, The average Ir–Ir bond length and average magnetic moment are 2.442 Å and $0.2\mu_b$/atom, respectively. These results are in accord with the previous theory results.[32]
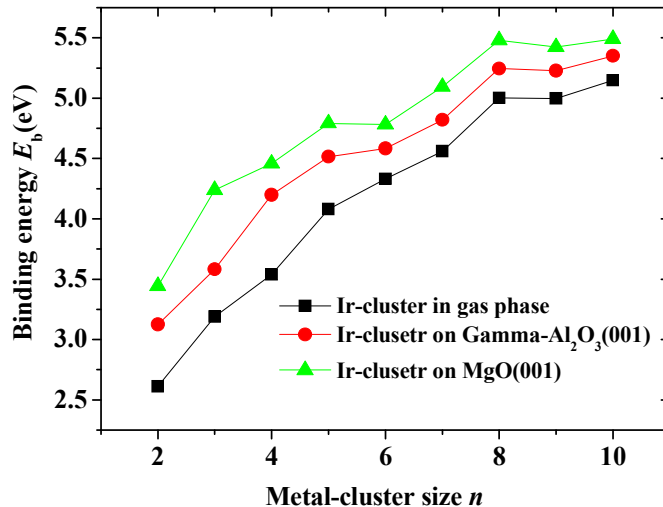
Figure 3. The average binding energies (E_b) of Ir_n(n=2-10) clusters as a function of cluster size.

From the above analysis, the average bond length ranged from 2.211 Å to 2.506 Å (see Table 1), which is not exceed the experimental bulk nearest-neighbor distance of 2.715 Å. As shown in Fig.3, we can see that

the calculated binding energy increases monotonically as cluster sizes increase.

3.2 Adsorption on γ-Al$_2$O$_3$(001) and MgO(100) Surface

Table 2. The Adsorption Energy(E_{ads}), Interaction Energy(E_{int}), Ir cluster Deformation Energy, E_{def}(Ir$_n$), Surface Deformation Energy($E_{def(surface)}$), Binding Energy(E_b/atom), Average Ir−Ir Bond Distances R$_{ave}$(Å) and Magnetic Moment (Mag) of Ir$_n$ Cluster on the γ-Al$_2$O$_3$(001) Surface and MgO(100) Surface.

n	E_{ads}(eV)		E_{int}(eV)		$E_{def(Irn)}$ (eV)		$E_{def(surface)}$ (eV)		E_b/atom(eV)		R_{ave}(Å)		Mag(μ_b)	
	γ-Al$_2$O$_3$	MgO	γ-Al$_2$O$_3$	MgO	γ-Al$_2$O$_3$	MgO	γ-Al$_2$O$_3$	MgO	γ-Al$_2$O$_3$	MgO	γ-Al$_2$O$_3$	MgO	γ-Al$_2$O$_3$	MgO
2	1.0274	1.6598	1.7278	2.5622	0.1401	0.2182	0.5603	0.6841	3.1269	3.4431	2.3010	2.3370	4	4
3	1.1741	3.1501	2.4533	3.9860	0.1228	0.1398	1.1563	0.6960	3.5818	4.2405	2.4290	2.4157	3	3
4	2.6454	3.6786	3.6786	4.1857	0.0004	-0.2214	0.9901	0.7285	4.1989	4.4572	2.4788	2.4360	0	2
5	2.1755	3.5529	3.1359	4.3986	0.0973	0.0666	0.8630	0.7790	4.5161	4.7915	2.4912	2.4865	1	3
6	0.8125	1.9886	3.6493	4.3426	0.9569	1.6854	0.7409	0.6685	4.5830	4.7810	2.5492	2.5364	2	4
7	1.8195	3.7318	2.6474	6.0590	0.0754	1.5190	0.7524	0.8080	4.8205	5.0937	2.5153	2.5281	7	1
8	1.9569	3.8374	2.9148	5.1991	0.2398	0.6951	0.7180	0.6665	5.2460	5.4810	2.467	2.4238	0	0
9	1.6441	3.8169	2.5067	5.0477	0.3409	0.5216	0.5216	0.7163	5.2271	5.4221	2.4252	2.4249	0	0
10	1.7821	3.4505	2.4739	4.8496	0.1326	0.5591	0.5591	0.8335	5.3499	5.4912	2.4492	2.4547	0	0

We firstly give a brief introduction of two support surface. As shown in Fig.1, the surface with octahedral Al atoms (denoted Al$_O$), tetrahedral Al atoms (denoted Al$_T$) and three-fold-coordinated O atoms are exposed, among which two kinds of O atoms at the surface layer can be found, with one bonded with the octahedral Al atoms only (denoted O$_O$) and

another bonded with both octahedral and tetrahedral Al atoms (denoted O_{OT}). On the MgO(100) surface, only one kind of five-fold-coordinated O atoms and Mg atoms at the surface layer. Secondly, we put the optimized Ir_n (n=2-10) cluster in its gas phase (see Fig.2) on the well-defined adsorption sites, and the most energetically preferred structures are shown in Fig.4 and Figu.5. The corresponding energies are listed in Table 2.

For single Ir adsorption, according to our previous work, we recalculated different adsorption sites, the results show that the energetically most favorable sites for the single Ir are the top sites of the O_{OT} atoms at the γ-Al_2O_3(001) surface and the top sites of the O atoms at the MgO (100) surface. The adsorption energy for Ir_1/γ-Al_2O_3(001) is predicted to be 0.126 eV lower than the Ir_1/MgO(100).

For Ir_2 cluster, as shown in Fig.4b, two Ir atoms occupied the O_{OT}-Al_O bridge site with Ir-O_{OT}, Ir-Al_O bond length of $\sim$2.34Å and 2.53 Å. The length of Ir_2 bond in the adsorbed Ir_2 cluster is enlarged to 2.301 Å from 2.211 Å in the gas phase. The most stable structure for MgO(100) is two Ir atoms adsorbed on the top sites of O atom(see Fig.5b). The bond length of adsorbed Ir_2 cluster is 2.337 Å. Adsorbate-induced surface relaxation on surpport has been observed. With increase of the surface deformation energy, the adsorption energy of Ir_2 cluster decreased.

As shown in Fig.4c, the most stable adsorption configuration of Ir_3 cluster lies aslant on the γ-Al_2O_3 (001) with Ir-O_{OT} bond length of 2.131

Å and 2.322 Å. While the most stable configuration for MgO(100) is a triangular Ir_3 vertical adsorbed on MgO(100) surface(see Fig.5c). The band lengths of Ir-O are 2.077 Å and 2.075 Å, respectively. The Ir_3-support interaction energy (3.986eV) is obviously large than that of γ-Al_2O_3 (001) surface.

The Ir_4 cluster interacts with γ-Al_2O_3 (001) surface via three triangular Ir atoms. As shown in Table 2, the adsorption energy is 2.6454eV, which is the strongest adsorption for Ir_n(n=2-10) cluster on γ-Al_2O_3 (001) surface. The magnetic moment remain as $0\mu_b$. Compared to the Ir_4 cluster on MgO (100) surface, the adsorption of Ir_4 cluster is accompanied by the very small cluster deformation with negligible energy of 0.0004eV. Moreover, in Fig.5d, we can see that the adsorption of Ir_4 cluster cleaves one of the Ir−Ir bonds in the gas phase with atomic magnetic moment of $2\mu_b$. This enhances the clusters interaction with the support at the cost of negative cluster deformation energy, which means the adsorbed Ir_4 cluster has been severely distorted.

For Ir_5 cluster, the most stable configuration of two surfaces is similar, and the Ir_5 cluster interacts with the surface via four Ir atoms bond to surface O atoms. The average band lengths of Ir-O on Ir_5/MgO(100) and Ir_5/γ-Al_2O_3 (001) is 2.225 Å and 2.320 Å, respectively.

In Fig.4f and Fig.5f, Ir_6 cluster interacts with the γ-Al_2O_3 (001) surface via three triangular Ir atoms bond to surface O atoms and Al

atoms, while on MgO(100) surface Ir$_6$ cluster via two Ir atoms connect directly with O atoms. Meanwhile, the adsorption energy of Ir$_6$ cluster decreased sharply. The Ir$_6$/MgO(100) and Ir$_6$/γ-Al$_2$O$_3$(001) cluster deformation energy are 0.9569 eV and 1.6854eV, respectively. The decrease of the adsorption energy for Ir$_6$ cluster is mainly due to the increase of Ir$_6$-support cluster deformation energy.

For Ir$_7$/MgO(100) adsorption, the interaction energy reach up to 6.059eV, which is the main contribution of the adsorption energy and far bigger than that of Ir$_7$/γ-Al$_2$O$_3$(001). Meanwhile, the Ir$_7$/γ-Al$_2$O$_3$(001) cluster deformation energy is only 0.0754 eV, which led to an increase of adsorption energy.

The adsorption energy of Ir$_8$/MgO(100) is 3.8374 eV, which is not only the strongest adsorption for Ir$_n$(n=2-10) cluster on MgO(100) surface but also double than that of Ir$_8$/γ -Al$_2$O$_3$(001). The average band lengths of Ir-O on Ir$_8$/MgO(100) and Ir$_8$/γ -Al$_2$O$_3$(001) is 2.194 Å and 2.264 Å, respectively.

Similar to the adsorption of Ir$_8$ cluster, the Ir$_9$ and Ir$_{10}$ cluster interact with the surface via four Ir atoms bond to surface four O atoms. The interaction energy of the Ir$_9$ and Ir$_{10}$ cluster is small than that of Ir$_8$ cluster. Meanwhile, compared with γ -Al$_2$O$_3$(001) surface, the interaction energy on MgO(100) surface is twofold increased.

Based on the above analysis, the average Ir-Ir distance and bonding

energy for Ir_n cluster in contact with the support is slightly larger than those for the free Ir_n clusters. In Tables 2 and Fig.3, we can see that the adsorption energy and binding energy of $Ir_n(n=2\text{-}10)/\gamma$ -$Al_2O_3(001)$ are lower than that of $Ir_n/MgO(100)$. The Magnetic Moment of Ir_n clusters in each most stable configuration vary from 0 to $7\mu_b$, depending on which oxides support is considered. Comparing with the gas phase cluster results listed in Table 1, we can see that most of the adsorbed Ir_n cluster changes its preferred spin state. However, the Ir_2, Ir_3 and Ir_8 clusters in gas phase and adsorbed clusters were found to have the same Magnetic Moment. Moreover, the strongest adsorption energy cluster for $\gamma\text{-}Al_2O_3(001)$ is the tetrahedral Ir_4 cluster, while $MgO(100)$ is cubic structure Ir_8 cluster.

(a) Ir$_1$

(b) Ir$_2$

(c) Ir$_3$

(d) Ir$_4$

(e) Ir$_5$

(f) Ir$_6$

(g) Ir$_7$

(h) Ir$_8$

(i) Ir$_9$

(j) Ir$_{10}$
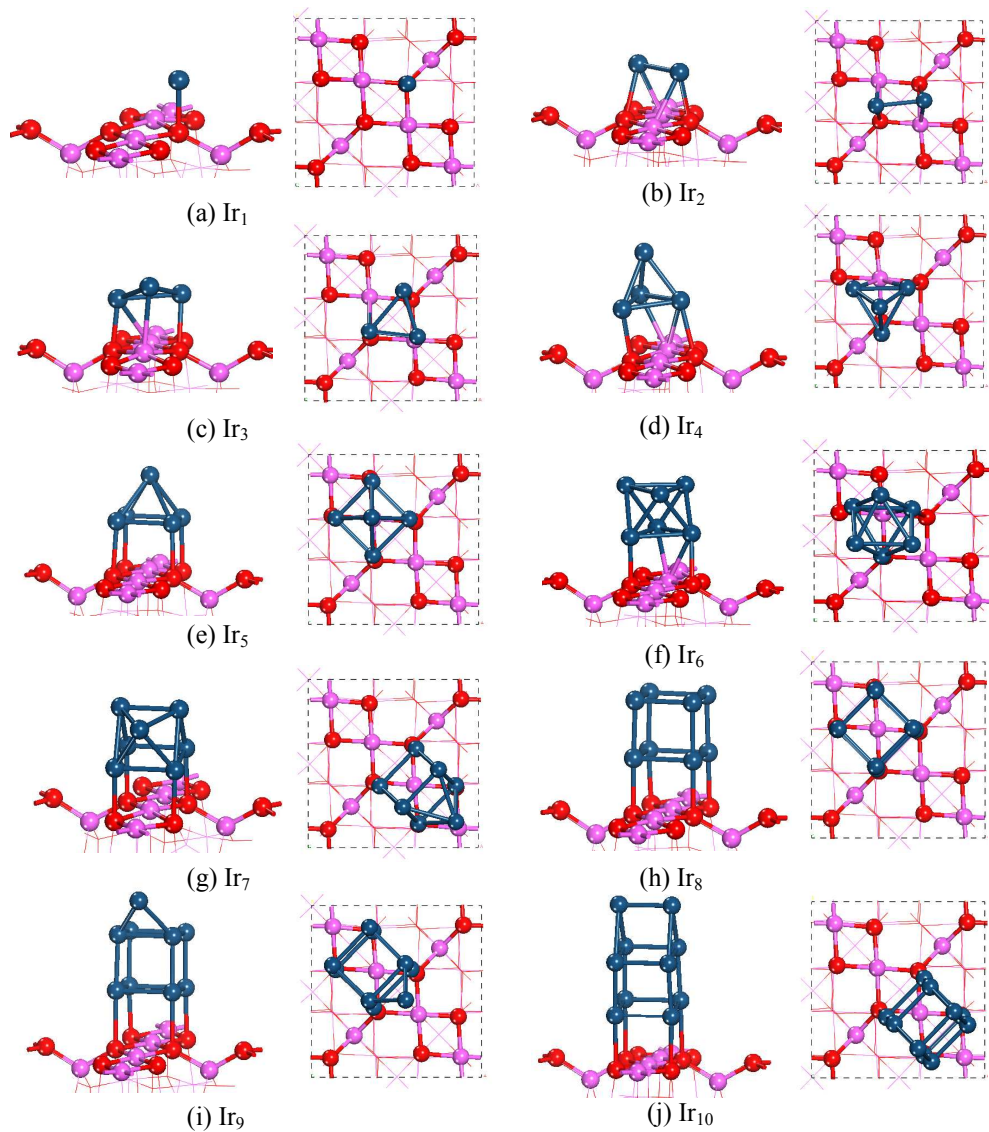
Figure 4. The most stable adsorption configuration of Ir$_n$(n=1–10) cluster on γ-Al$_2$O$_3$(001) surface. The red, pink, and atrovirens spheres represent O, Al and Ir atoms, respectively.
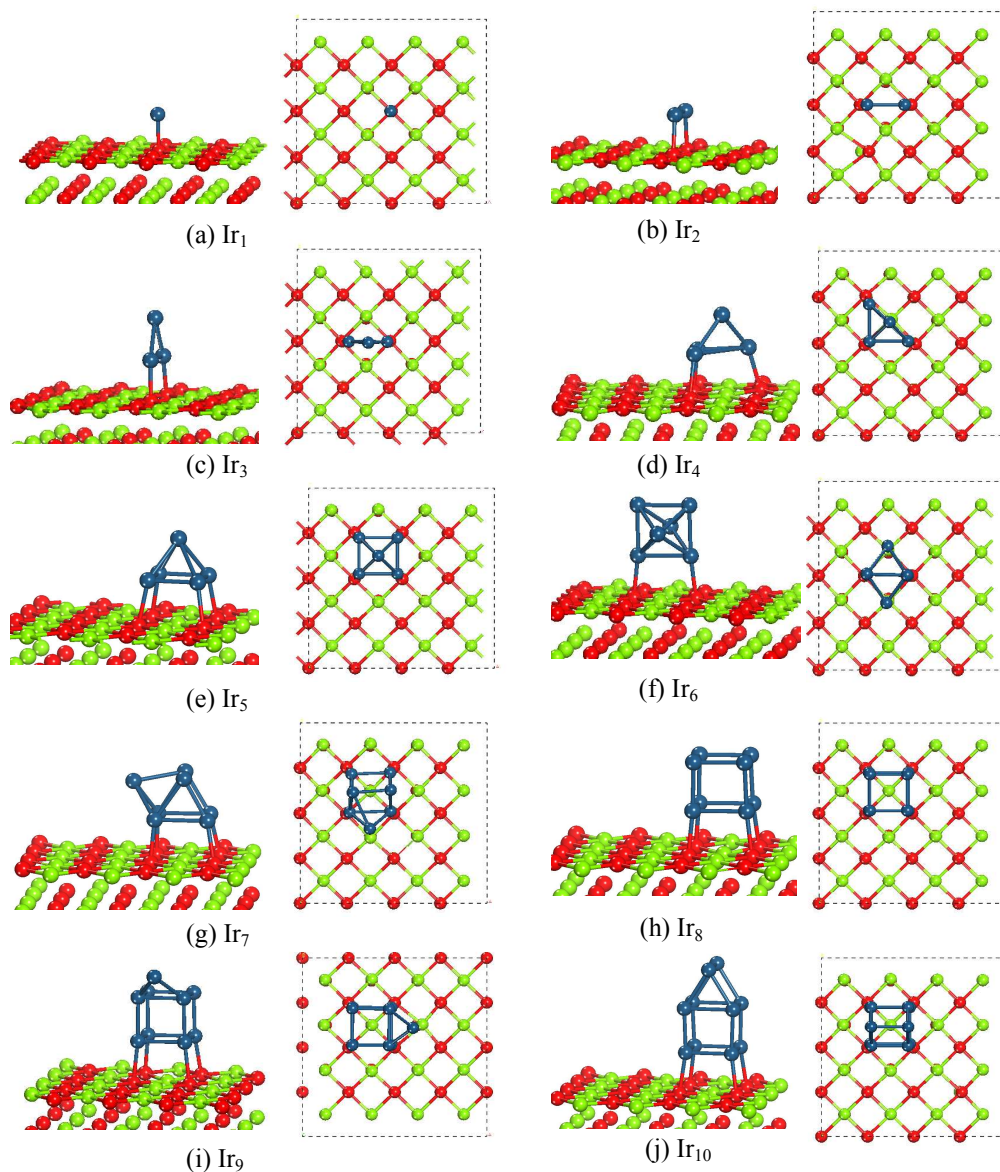
Figure 5. The most stable adsorption configuration of Ir_n ($n=1-10$) cluster on MgO(100) surface. The red, green and atrovirens spheres represent O, Mg and Ir atoms, respectively.

3.3 Nucleation of Ir_n Cluster on the γ-Al_2O_3(001) and MgO(100) Surfaces

To further understand the properties of Ir_n clusters, we investigated the nucleation of Ir_2-Ir_{10} clusters on the γ-Al_2O_3(001) and MgO(100) Surfaces. The nucleation energy can be defined as following equation:

$$E_{nuc}=E(Ir_n/slab)+E(slab)-E(Ir_{n-1}/slab)-E(Ir_1/slab) \qquad (8)$$

Where $E(Ir_n/slab)$ is the total energy of Ir_n cluster deposited on slab, and $E(slab)$ is the total energy of slab. Based on the above energetically configurations, the nucleation energies on each surface are listed in Table 3 and Fig.6.

Table 3 The nucleation energy E_{nuc} of $Ir_n(n=2–10)$ cluster deposited on the γ-Al$_2$O$_3$(001) surface, MgO(100) surface and the $Ir_n(n=2–10)$ cluster in gas phase.

n	E_{nuc}/(eV)		
	Gas phase	γ-Al$_2$O$_3$(001)	MgO(100)
2	-5.2264	-2.7690	-2.5231
3	-4.3449	-2.7493	-3.6536
4	-4.5789	-4.3078	-2.5568
5	-6.2546	-4.0423	-3.9474
6	-5.5909	-3.1896	-4.5033
7	-5.9281	-4.4389	-4.7856
8	-8.0871	-6.4821	-6.0112
9	-4.9709	-3.3341	-2.7688
10	-6.4800	-4.7127	-3.9321

As shown in Table 3, the negative values indicate that the nucleation of Ir_n cluster is exothermic, and thermodynamically favorable, while the positive value represent opposite. Obviously, the nucleation of Ir_n (n=2-10) cluster on both surface are thermodynamically favorable and exothermic, which indicate that the critical cluster size for Ir_n cluster nucleation on the γ-Al$_2$O$_3$(001) or MgO(100) surface surface is 2. However, the exothermicity is still lower than for gas phase clusters. The nucleation energy of $Ir_n(n$=2-10) cluster on the γ-Al$_2$O$_3$(001) surface is close to the corresponding energy on the MgO(100) surface, except for Ir_3, Ir_4 and Ir_6 cluster. Interestingly, the nucleation of Ir_3 and Ir_6 cluster on MgO(100) surface are more favorable than that on the γ-Al$_2$O$_3$(001) surface, while

the nucleation of Ir_4 cluster is reverse. Moreover, the nucleation energy of Ir_4 on γ-Al_2O_3 (001) surface is not only predicted to be 1.751eV low than corresponding energy on MgO(100) surface but also very close to the gas phase Ir_4 cluster.
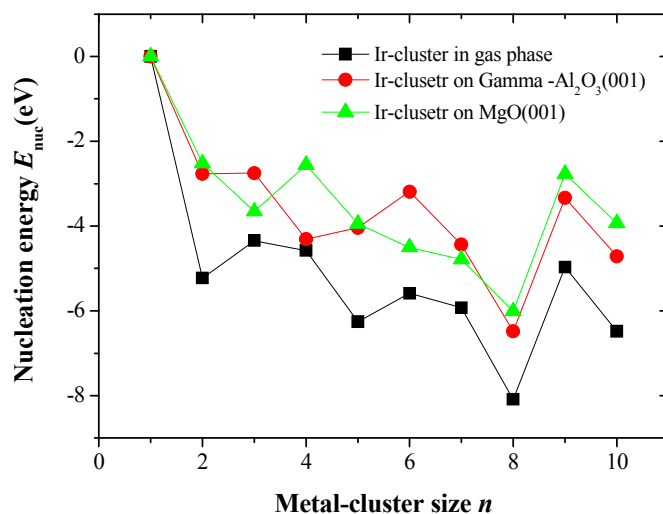
Figure 6. Nucleation energies E_{nuc} of gas phase Ir_n cluster, Ir_n on the γ-Al_2O_3(001) surface, Ir_n on the MgO(100) surface

3.4 Analysis of Charge Density

To have a direct view of the charge chemical bonding between Ir_n cluster and the different substrate, charge density analysis is also necessary. The spatial charge transfer within the Ir_n cluster could be important in the catalytic activity. Fig.7 gives the induced charge density of the Ir_4 adsorbed γ -Al_2O_3 (001) and MgO(100) surface, which is defined as the difference between the charge density of the Ir_4 adsorbed slab and the sum of the charge density of the bare slab with deformed

geometry after adsorption and the Ir_4 cluster in the same geometry. The equation can be defined as following:

$$\Delta\rho = \rho[Ir_4/slab] - \rho[slab] - \rho[Ir_4] \tag{9}$$

From above definition, the negative value (transparent yellow in Fig.7) of the iso-surface indicates that the atom losses charge while the positive value (transparent blue in Fig.7) indicates that the atom gains charge.
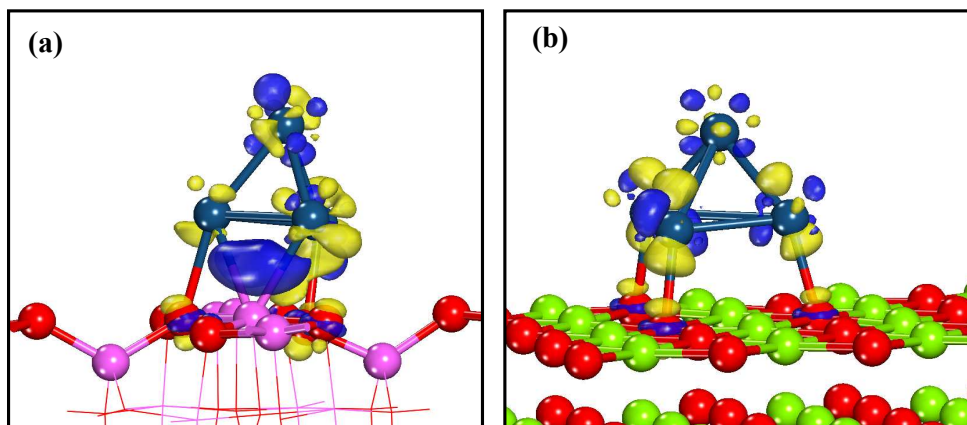
Figure 7. Induced charge density of the Ir_4 adsorbed on γ-Al_2O_3 (001) (a) and MgO(100) (b) surface. The red, pink, green and atrovirens spheres represent O, Al, Mg and Ir atoms, respectively. The iso-surfaces of the induced charge density (isovalue = 0.002) are in transparent blue (positive) and yellow (negative).

As shown in Fig.7, the Ir_4 cluster losses charge in some Ir orbitals. This depletion is balanced by an increase of the electron density of the Ir−Al bond and O atom located under the adsorbed Ir atom. Valero et al.[36] also found Pd-$4d$ orbital loss charge on the surface that is balanced by a significant increase of the charge density on the Pd−Al bond. On the MgO(100) surface, the Ir_4 cluster adsorbed directly on three O atoms. The induced charge density revealed that Ir-$5d$ orbital loss charge. However, this depletion is only balanced by an increase of the charge density of the

Ir-O region.

To have a better understanding of the Ir_4 cluster on different support, the projected density of states (PDOS) have been calculated. The PDOS of Ir-$5d$ states for different condition are compared in Fig.8.
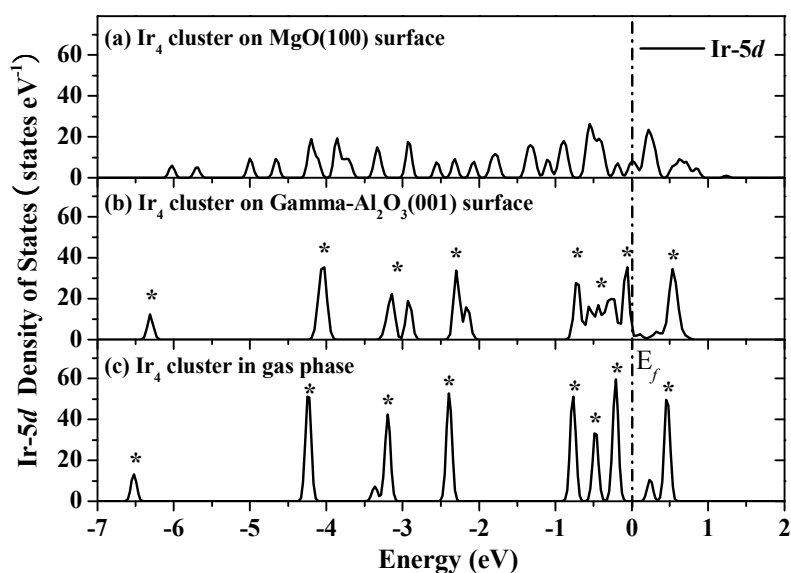
Figure 8. Total density of states for the Ir-$5d$ states on the MgO(100), γ -Al$_2$O$_3$ (001) surface and for an isolated Ir$_4$ cluster in gas phase

From Fig.8 we can see that the Ir-$5d$ states move up and cross the Fermi level after the Ir$_4$ cluster deposited on support. Some of those states becoming unoccupied, which means the Ir$_4$ cluster losses charge. Comparing the Fig.8a and Fig.8b, it is clearly that the electronic states of Ir$_4$ cluster on MgO(100) have been changed significantly, while the Ir$_4$ cluster on γ -Al$_2$O$_3$ (001) still maintained its initial state. Moreover, by comparing the characteristic peak in Fig.8b and Fig.8c, besides minor differences, the shape of the PDOS for Ir$_4$ cluster on γ -Al$_2$O$_3$ (001) and

Ir_4 cluster in gas phase are basically similar, which is in accordance with the deformation energy of Ir_4 cluster deposited on γ-Al_2O_3 (001).

4. CONCLUSIONS

First principles DFT calculations based on periodic supercell models were employed to investigate the structural, stability, and magnetic properties of iridium clusters Ir_n ($n=2-10$) and its interaction on γ-Al_2O_3 (001) and MgO(100) Surface. Our results show that the adsorption energy and binding energy of Ir_n cluster on γ-Al_2O_3(001) are lower than that on MgO(100), suggesting that the adsorbed Ir_n ($n=2-10$) cluster are much more stably on the MgO(100) surface than the corresponding cluster on the γ-Al_2O_3(001) surface. Moreover, the strongest adsorption energy cluster for γ-Al_2O_3(001) is the tetrahedral cluster, while MgO(100) is a cubic structure Ir_8 cluster. Therefore, the Ir_4/γ-Al_2O_3(001) and Ir_8/MgO(100) are expected to have high chemical reactivity in further experimental applications as catalyst.

The critical cluster size for Ir cluster nucleation on the γ-Al_2O_3(001) or MgO(100) surfaces is 2. Moreover, the nucleation energy of Ir_n($n=2-10$) cluster on the γ-Al_2O_3(001) surface is close to the corresponding energy on the MgO(100) surface, except for Ir_3, Ir_4 and Ir_6 cluster. Interestingly, the nucleation of Ir_3 and Ir_6 cluster on MgO(100) surface are more favorable than that on the γ-Al_2O_3(001) surface, while the nucleation of Ir_4 cluster is reverse and very close to the gas phase Ir_4 cluster.

Analysis of the induced charge density and density of state show that the adsorbed Ir_4 cluster on the γ-$Al_2O_3(001)$ surface has obviously charge transfer between Ir atoms and terminal Al, O atoms with negligible deformation. However, for the $MgO(100)$ surface, the adsorbed Ir_4 cluster are severely distorted and bind directly to three surface O atoms. This result may be useful to understand the previous experiment, where Argo et al observed the catalytic activity of the iridium clusters for alkene hydrogenation reactions is tenfold boosted when γ-Al_2O_3 is used to instead of MgO.

References

[1] G. Ertl, H. Knozinger, J. Weitkamp, *Handbook of Heterogeneous Catalysis*, Wiley Company, Weinheim, 1997.

[2] M. Boudart, *J. Mol. Catal,* 1985, **30**, 27.

[3] B.C. Gates, *J. Mol. Catal. A: Chem,* 2000, **163**, 55.

[4] J. F. Goellner, J. Guzman and B. C. Gates, *J. Phys. Chem. B,* 2003, **106**, 1229.

[5] S. D. Maloney, F. B. M. van Zon, M. J. Kelley, D. C. Koningsberger, B. C. Gates, *Catal. Lett,*1990, **5**, 161.

[6] S. Kawi, B. C. Gates, *Inorg. Chem.,* 1992, **31**, 2939.

[7] O. Alexeev, G. Panjabi, B. C. Gates, *J. Catal.*, 1998, **173**, 196.

[8] A. Zhao, B. C. Gates, *J. Am. Chem. Soc.*, 1996, **118**, 2458.

[9] M. Aizawa, S. Lee, S. L. Anderson, *Surf. Sci.*, 2003, **253**, 542.

[10] A. M. Argo, J. F. Odzak, J. F. Goellner, F. S. Lai, F. S. Xiao, B. C. Gates, *J. Phys.Chem. B*, 2006, **110**, 1775-1786.

[11] B.C. Gates. *J. Mol. Catal. A: Chem,* 2000, **163**, 55.

[12] A.M. Argo, J.F. Odzak, F.S. Lai, B.C. Gates, *Nature*, 2002, **415**, 632.

[13] N. S. Babu, N. Lingaiah, R. Gopinath, P. S. S. Reddy, P. S. S. Prasad, *J. Phys. Chem. C* 2007, **111**, 6447.

[14] D. C. Meier, D. W. Goodman, *J. Am. Chem. Soc.* 2004, **126**, 1892.

[15] R. Gopinath, N. S. Babu, J. V. Kumar, N. Lingaiah, P. S. S. Prasad, *Catal. Lett.* 2008, **120**, 312.

[16] N. C. Hernandez, J. Graciani, A. Marquez, J. F. Sanz, *Surf. Sci.*, 2005, **575**, 189.

[17] N. C. Hernández, A. Márquez, J. F. Sanz, J. R. B. Gomes, F. Illas, *J. Phys. Chem. B*, 2004, **108**, 15671.

[18] L. G. V. Briquet, C. R. A. Catlow, S. A. French, *J. Phys. Chem. C*, 2008, **112**, 18948.

[19] Y. C. Chen，L. J. Song, Z. L. Sun, *Physics Letters A*, 2012, **376**, 1919.

[20] M. C. Valero, P. Raybaud, P. Sautet, *Phys. Rev. B*, 2007, **75**, 045427.

[21] X. R. Shi, D. S. Sholl, *J. Phys. Chem. C*, 2012, **116**, 10623-10631.

[22] J. R. Li, R. G. Zhang, B. J. Wang, *Appl. Surf. Sci.*, 2013, **270**, 728.

[23] G. Kresse, Hafner, *Phys. Rev. B.*, 1993, **47**, 558.

[24] G. Kresse, Furthmuller. *J. Computational Materials Science* 1996, **6**, 15.

[25] P. E. Blöchl, *Phys. Rev. B.*, 1994, **50**, 17953-17979.

[26] Y.C. Chen, C.Y. Ouyang, S.Q. Shi, Z.L. Sun, L. Song, *Phys. Lett. A*, 2009, **373**,277.

[27] H. J. Monkhorst, J. D. Pack, *Phys. Rev. B.*, 1976, **13**, 5188.

[28] T. Pawluk, Y. Hirata, L. C. Wang, *J. Phys. Chem. B*, 2005, **109**, 20817.

[29] J. L. Jules, J. R. Lombardi, *J. Phys. Chem. A*, 2003, **107**, 1268.

[30] M. Castro, C. Jamorski, D. R. Salahub, *Chem. Phys. Lett.*, 1997, **271**, 133.

[31]Z. Xu, F.S. Xiao, S.K. Pumell, O. Aiexeev, S. Kawi, S.E.Deutsch, B.C. Gates, *Nature*, 1994, **372**, 346.

[32]J. G. Du, X. Y. Sun, J Chen, G Jiang, *J. Phys. Chem. A*,2010, **114**, 12825.

[33]S. D. Maloney, EB.M. van Zon, M.J. Kelley, D.C. Koningsberger, B.C. Gates, *Catal. Lett.*, 1990, **5**, 161.

[34]M. Y. Chen and A. David, *J. Phys. Chem. A*, 2013, **117**, 3676.

[35]W. Q. Zhang, L. Xiao, Y. Hirata, T. Pawluk, L. C. Wang, *Chem. Phys. Lett.* 2004, **383**, 67.

[36]M. C. Valero, P. Raybaud, P. Sautet, *Phys. Rev. B* 2007, **75**, 045427.